Flow Lithography

DOI: 10.1002/anie.200905229

Hydrodynamic Focusing Lithography**

*Ki Wan Bong, Ki Tae Bong, Daniel C. Pregibon, and Patrick S. Doyle**

Anisotropic multifunctional particles hold great promise for drug delivery,[1] imaging,[2] and construction of building blocks[3,4] for dynamic mesostructures such as self-assembled tissues[4,5] and 3-D electrical circuits.[6] Of particular interest, multifunctional particles with unique barcodes have been suggested as diagnosis tools for rapid screening of biomolecules.[7] For these applications, particle design is at least as important as size[3,7–10] and requires a fabrication technique with precise control over shape and chemical patchiness. Methods currently used to generate multifunctional particles include microcutting,[11] co-jetting,[12] core–shell systems,[13] photo resist-based lithography,[14] and the PRINT method (particle replication in non-wetting templates).[15] The morphology of particles prepared by co-jetting, microcutting, and core–shell systems has been limited to spheres and cylinders.[11–13] Although multilayer lithography overcomes this limitation,[14] the use of photoresist materials renders this approach suboptimal for many applications.

While the PRINT method[15] has its strength in producing small sub-μm particles, to date multiphasic particles beyond a 1-D stripe have not been synthesized. Furthermore, during multifunctional particle synthesis, the technique needs multiple steps and does not provide flexibility as particle shapes are restricted to the pre-defined stamping molds.

Previously, we have shown that flow lithography (FL) can be used to generate multifunctional particles—we exploited several microfluidic characteristics such as co-flow of liquid monomers, rapid fluidic exchange, and simple controllability.[16–19] In FL, we can use a combination of adjacent flowing photocurable monomers with lithographic masks to simultaneously define the shape and chemical pattern of particles.[16] Recently, we also developed lock release lithography (LRL)[19] to extend chemical patterning to multiple dimensions. However, these FL-based approaches for generating particles with patterned chemistries require precise alignment of masks at flow interfaces and concomitant modest particle throughput. Currently, FL cannot be used to synthesize multifunctional particles with chemical anisotropy in the channel height direction (z direction in this article, c.f. Figure 1 A).

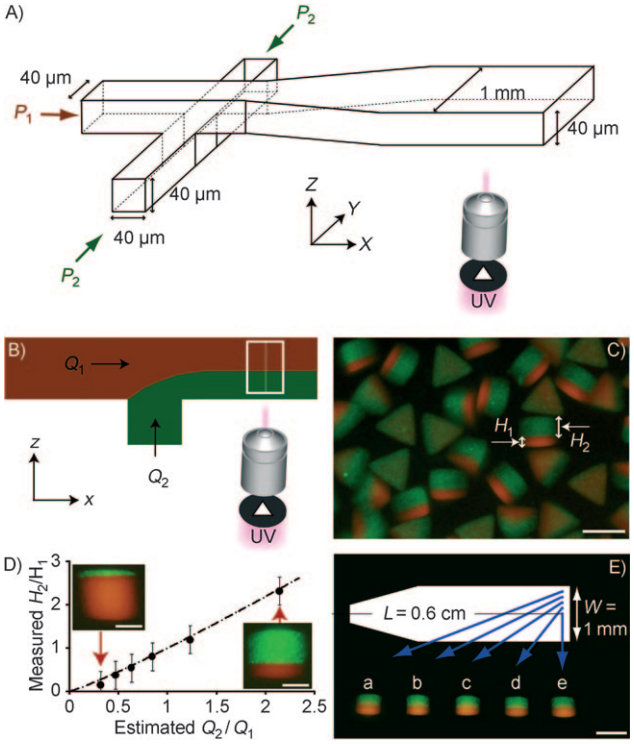

Figure 1. Hydrodynamic focusing lithography (HFL) for high-throughput synthesis of Janus microparticles. A) Microfluidic device used in HFL. P_1 and P_2 represent the inlet pressures of top and bottom channel respectively. All inlet dimensions are 40×40 μm. Particles are synthesized after layered flows are widened up to 1 mm in a 40 μm tall region of the channel. B) A side view of flow focusing and particle polymerization. C) A fluorescent image of 50 μm triangular particles with green (200 nm, green fluorescent beads) and red (rhodamine A) layers. H_1 and H_2 are the heights of top (red) and bottom (green) layer in a particle. D) Comparison of measured H_2/H_1 versus estimated flow ratio Q_2/Q_1 (see Supporting Information). The dashed line is the prediction from a hydrodynamic model (Eq. (12) in Supporting Information). E) Uniformity of Janus particles synthesized at a, b, c, d, and e spots across a 1 mm width channel. The intervals between spots are 100 μm. Scale bars are 50 μm (C,E) and 20 μm (D).

Here, we introduce a new method called hydrodynamic focusing lithography (HFL) that harnesses flow focusing to create stacked flows in two-layered channels for particle synthesis. Contrary to our prior methods to create multilayered particles, here the fluid interface can be perpendicular to the UV light propagation direction and precise mask alignment at the interface is no longer needed. This change in geometry also allows us to polymerize 2-D arrays, compared to 1-D in the prior method, which can increase throughput substantially. In HFL, multiple monomer streams can be simultaneously stacked in both the z and y direction leading to more complex particles than before. Finally, we demon-

[*] K. W. Bong, K. T. Bong, D. C. Pregibon, Prof. P. S. Doyle
Department of Chemical Engineering
Massachusetts Institute of Technology
77 Massachusetts Avenue, Cambridge, MA 02139 (USA)
E-mail: pdoyle@mit.edu
Homepage: http://web.mit.edu/doylegroup

[**] We gratefully acknowledge the support of Kwanjeong Educational Foundation, the MIT Deshpande Center, and the Singapore–MIT Alliance. We also thank S. C. Chapin, M. Aquing, P. Panda, and R. Haghgooie for useful discussions.

Supporting information for this article is available on the WWW under http://dx.doi.org/10.1002/anie.200905229.

strate that particles prepared by HFL can be combined with capture proteins on selected layers.

Flow lithography is made possible by the presence of a lubrication layer at the channel walls, which results from the quenching of free-radical reactions at the channel walls by oxygen that has diffused through the polydimethylsiloxane (PDMS).[20] Typically, two-layered PDMS devices are irreversibly sealed using oxygen plasma activation.[21,22] However, the activated surfaces covered with silanol groups are less permeable to oxygen, diminishing the presence of a suitable lubrication layer. Although PDMS sacrificial layers could be used during plasma treatment to avoid oxidizing specific regions of the devices, the method leads to imperfect sealing with the potential of leaking. We observed that layered flows in these devices were frequently mixed as a result of leaking. Alternatively, channels can be sealed using the technique of partial curing, device fabrication, and complete curing. We used a PDMS–polyurethane acrylate (PUA)–PDMS replica molding technique[23] to prepare a partially cured bottom PDMS channels on a glass slide (for details, see Supporting Information). This method is preferred when fabricating gas permeable two-layered PDMS channels for flow lithography.

Figure 1 A shows a typical channel used for particle synthesis. Narrow channels (40 μm) were used to minimize mixing as stacked streams were introduced, providing stable layered flows in the z direction.[21,22] Further along the channel, the flows are widened up to 1 mm for particle synthesis. Like other flow lithography techniques,[16–19] HFL can be applied to a broad range of precursor materials. We typically use monomers based on poly(ethylene glycol) (PEG) that are bio-friendly, and can be functionalized with a variety of biomolecules. As the prepolymer solutions we employ here are miscible, we can neglect the effect of surface tension between layered flows.

To mass-produce layered particles in two-layered PDMS channels, we used stop flow lithography (SFL).[17] This automated, cyclic process allows flow stoppage, then particle polymerization, and subsequent flow. SFL has three main advantages for the synthesis of multifunctional particles with respect to throughput, resolution, and sharpness of interfaces.[17] However, during multifunctional particle synthesis, traditional SFL requires precise mask alignment across the interface and each synthesis step polymerizes only 1-D rows of particles. The change in orientation of the fluid interface in HFL allows for production of 2-D arrays in each step. With a circular polymerization region of radius D and a particle dimension L, synthesis throughput per cycle is approximately $\pi D^2/4L^2$ for a 2-D array of particles in comparison to D/L for a single row. In our current setup, D is approximately 1 mm, and taking a particle dimension of 5 μm, the throughput is increased by more than 200×. Furthermore, resolution of layer heights is now controlled by automated flow rather than manual mask alignment.

To demonstrate an application of HFL, we synthesized bifunctional, triangular PEG particles comprised of an upper layer with rhodamine acrylate and a bottom layer containing 200 nm green fluorescent beads (Figure 1 B,C). The relative thickness of each chemical region, H_1 and H_2, could be readily controlled by adjusting the ratio of inlet pressures. In our plots, we used estimated volumetric flow rates instead of inlet pressures due to ease of presentation. We recall that HFL (and SFL) can quickly stop and start the flows (polymerizing features in the stop regime) because they control pressure at the inputs, whereas sources that directly control flow rates (e.g. syringe pumps) typically have a slow response time. We derived a relation between the inlet pressures P and estimated flow rates Q in the polymerization region. The a priori prediction from a simple model (see Supporting Information) is shown as the dashed curve in Figure 1 D and compares well with the experiments. When the height of each flow stream is much larger than the oxygen inhibition layer thickness, the model reduces to $H_2/H_1 \approx Q_2/Q_1$. We were able to precisely tune a single layer height from 32 to ca. 4.5 μm.

We also demonstrated that during synthesis with HFL, particles with uniform dimensions are generated across the channel width. It is known that PDMS channels deflect under pressure-driven flows, giving a local channel height that is dependent on the position.[24] In this view, continuous flow lithography (CFL)[16] is not compatible with HFL as layer thicknesses will be different at each location. However, SFL can be used to yield uniform layered particles without position dependency since polymerization occurs at zero applied pressure, after the PDMS channel has recovered from a deflected state—as long as the stop time (t_s) is longer than the time required for channel relaxation (t_r). The relaxation time is dependent on channel width, channel height, viscosity of the solution, and distances from inlets.[17] At 0.6 cm downstream in a 1 mm wide channel with 40 μm heights, t_r is estimated to be 0.07 s.[17] Also, the polymerization time (t_p) should be kept to a minimum in order to prevent species diffusion between layers. Using t_r of 300 ms and t_p of 50 ms, we showed that layered particles with uniform features were generated across the channel width (Figure 1 E).

We showed that multiple flows can be stacked by increasing the number of inlets entering sequentially from the bottom layer of the device (Figure 2 A). Using such multiflow stacking, we synthesized triangular particles containing three layers (Figure 2 B,C). The aspect ratio of these trilayered particles is defined to be the ratio of the overall particle height divided by the size of the feature produced by the transparency mask. Using variations of mask feature sizes in similar channels, we generated particles with aspect ratios greater than (Figure 2 D) or less than 1 (Figure 2 E).

As perhaps the most valuable feature of HFL, the method can also be used for high-throughput synthesis of dual-axis multifunctional particles with mask-defined morphologies. Such particles have not previously been made in microfluidic devices. We generate a 2-D flow focusing[25] geometry by first co-flowing monomers F1 (PEGDA, poly(ethylene glycol) diacrylate, with rhodamine A) and F2 (PEGDA with 100 nm blue fluorescent beads) using two inlets of top channel (Figure 3 A). This flow is then stacked on monomer F3 (PEGDA with 200 nm green fluorescent beads), which enters from the bottom channel. Shown in Figure 3 C,D are the layered flows that comprise the top (flow 1 and flow 2) and bottom layers (flow 3). Using a transparency mask with a single row of features, we synthesized cross-shaped particles with dual-axis functionality at the interface of flows (Fig-

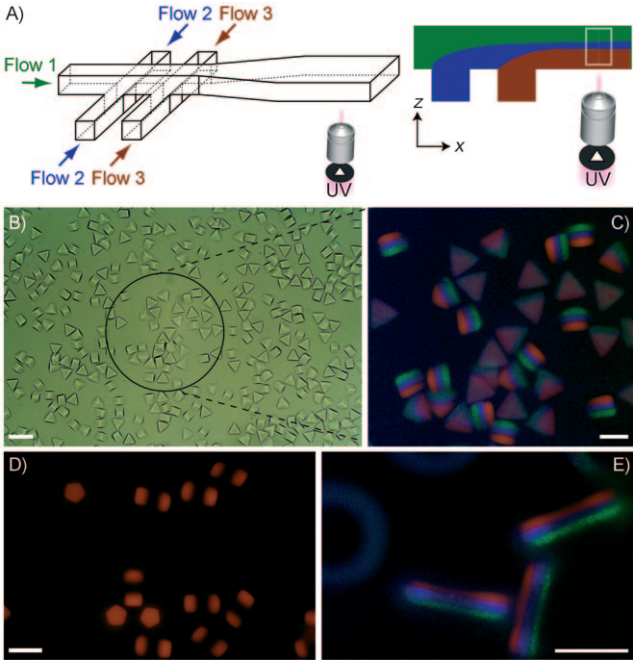

Figure 2. High-throughput synthesis of multilayered microparticles. A) Synthesis process of trilayered microparticles. For three-flow stacking, flow 1 (PEGDA with 200 nm green fluorescent beads) is combined with flow 2 (PEGDA with 100 nm blue fluorescent beads) and flow 3 (PEGDA with rhodamine A) entering sequentially from the bottom layer of the device. In the stable layered flow, triphasic triangular particles can be synthesized using a mask with triangles. B) Differential interference contrast (DIC) image of 50 μm trilayered triangular particles. C) Magnified fluorescent image for the circled region of (B). D) 20 μm pentagonal particles with aspect ratio 2. These particles contain rhodamine A in both top and bottom layers but no fluorophores in the middle layer. E) 150 μm trilayered ring particles with aspect ratio 0.25. Scale bars are 100 μm (B,E), 50 μm (C), and 30 μm (D).

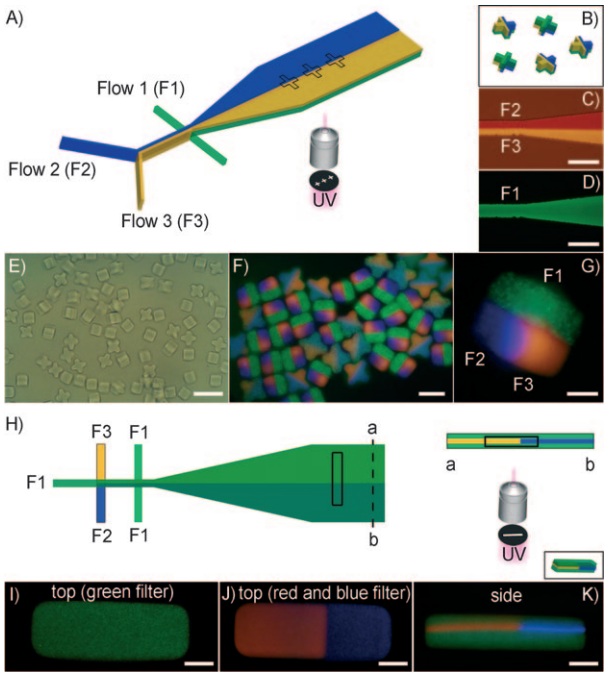

Figure 3. Synthesis of dual-axis layered microparticles. A,B) Synthesis process of dual-axis layered microparticles. Flow 1 (F1), flow 2 (F2), and flow 3 (F3) contain 200 nm green fluorescent beads, 100 nm blue fluorescent beads, and rhodamine A as fluorophores, respectively. C,D) Fluorescent images (red filter in (C) and green filter in (D)) of dual-axis flows in a two-layered PDMS channel. E) DIC image of 40 μm cross shaped particles with red, blue (in top), and green layers (in bottom). F) A fluorescent image of particles shown in (E). G) A side view of a particle shown in (F). H) Synthesis process of four-layered sandwich particles with dual layers in the middle. a–b is the intersection of the channel with dual-axis four-layered flows. I–K) Fluorescent images of sandwich particles generated by the process in (H). Scale bars are 80 μm (C,D,E), 50 μm (I,J,K), 40 μm (F), and 10 μm (G).

ure 3E–G). Although the production rate for this process is similar to that of traditional SFL due to the necessity of 1-D row synthesis, the process extends the degree of freedom for chemical anisotropy in a particle to two dimensions.

Using this process, virtually any number of flows can be stacked. To demonstrate this, we generated particles which contain in their center side-by-side stacked monomers which are bounded on the top and bottom by a third monomer stream (Figure 3H). To achieve this, flow 3 was introduced in at both the top and second bottom channel, while the monomers contained in the middle layer were combined at the first bottom inlet. Using a mask of rectangular shapes with rounded corners, we synthesized sandwich-like multifunctional particles at the interface of the two flows in the middle layer (Figure 3H,K). As shown in Figure 3I,J, the sandwich particles had green fluorescent top and bottom layers (Figure 3I) with red and blue fluorescent layers comprising the middle (Figure 3J). For such dual-axis particles, chemical anisotropy in the y direction can be controlled by mask alignments at the flow interface.

Finally, we demonstrate that particles prepared by HFL can be patterned with proteins on a specific layer. These "caps" can be used to restrict target capture to specific particle faces (Figure 4A.) To achieve protein capturing, we first synthesized biotin–PEG-acrylate (PEGA) by preparing a 1:1 molar mixture of biotin hydrazide and PEGA-succinimidyl ester in commercial 1× phosphate buffered saline (PBS) and used this as an anchor to attach streptavidin. This allows us to directly copolymerize biotin in a selected region of the particle. The trilayer flow is shown in Figure 4A, and the acrylated biotin is in the center flow. The resulting synthesized triangular particles are shown in Figure 4B. Next, streptavidin–Cy3 was incubated with the particles at 37 °C for 30 min. The streptavidin–Cy3 will strongly associate with the biotin. As the size of streptavidin (≈5 nm) was bigger than the porosity size of the hydrogel networks,[19,26] the proteins could not penetrate the gel structures, resulting in the coatings on sides of particles. In Figure 4C, the fluorescence pattern indicates that proteins were not bound to top and bottom layers. Furthermore, the resulting specific association shows that the biotin is still active after UV polymerization, akin to our prior work with nucleic acids.[7] The short UV exposure dose required for synthesis is the most likely reason that bioactivity is retained.

We have presented a new technique called hydrodynamic focusing lithography (HFL) that combines flow-stacking and

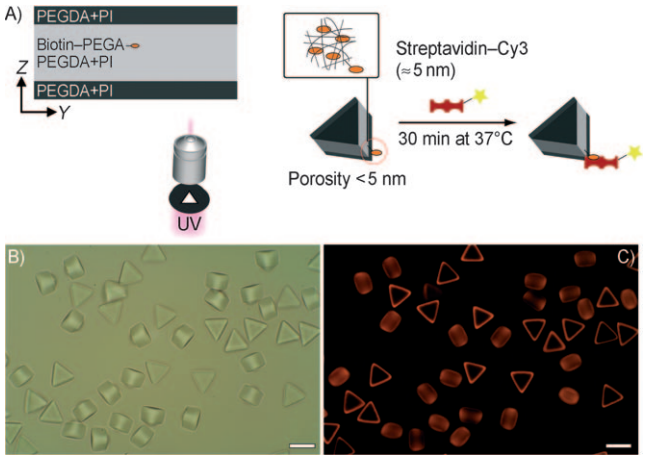

Figure 4. Protein conjugation on selected regions. A) Preparation of triangular particles with patterned protein coatings. The middle flow contains biotin–PEGA (poly(ethylene glycol) acrylate) that is copolymerized in the particle. After incubation, the triangular particles are coated with streptavidin–Cy3 on the sides (PI: photoinitiator). B) A DIC image of the protein coated triangular particles. C) A fluorescent image of (B). All scale bars are 50 μm.

microfluidic particle synthesis. In HFL, the layered flows can be used to introduce chemical anisotropy in z direction of particles. For certain applications, the approach can increase the throughput of multifunctional particle synthesis over 200 times when compared to traditional stop-flow-lithography. We have also demonstrated that HFL can be used to produce dual-axis layered particles. HFL is a compelling method as the technique is compatible with other flow lithographic methods such as LRL[19] and stop flow interference lithography (SFIL).[18] For example, the combination of HFL and LRL can lead to chemical patterning in all dimensions as LRL can provide chemical anisotropy of particles in x–y dimension.[19] We believe that HFL can provide a powerful way to reach new complex particles.

Experimental Section

Details of the microfluidic device, the model to predict Q_2/Q_1 and H_2/H_1, materials, the stop-flow lithography setup, and other details are given in Supporting Information.

Received: September 18, 2009
Published online: November 30, 2009

Keywords: hydrogels · lithography · multifunctional materials · polymerization

[1] D. A. LaVan, T. McGuire, R. Langer, *Nat. Biotechnol.* **2003**, *21*, 1184.
[2] A. Walther, A. H. E. Müller, *Soft Matter* **2008**, *4*, 663.
[3] S. C. Glotzer, M. J. Solomon, *Nat. Mater.* **2007**, *6*, 557.
[4] R. S. Kane, *Angew. Chem.* **2008**, *120*, 1388; *Angew. Chem. Int. Ed.* **2008**, *47*, 1368.
[5] Y. A. Du, E. Lo, S. Ali, A. Khademhosseini, *Proc. Natl. Acad. Sci. USA* **2008**, *105*, 9522.
[6] D. H. Gracias, J. Tien, T. L. Breen, C. Hsu, G. M. Whitesides, *Science* **2000**, *289*, 1170.
[7] D. C. Pregibon, M. Toner, P. S. Doyle, *Science* **2007**, *315*, 1393.
[8] Y. Geng, P. Dalhaimer, S. S. Cai, R. Tsai, M. Tewari, T. Minko, D. E. Discher, *Nat. Nanotechnol.* **2007**, *2*, 249.
[9] J. A. Champion, S. Mitragotri, *Proc. Natl. Acad. Sci. USA* **2006**, *103*, 4930.
[10] S. E. A. Gratton, P. A. Ropp, P. D. Pohlhaus, J. C. Luft, V. J. Madden, M. E. Napier, J. M. DeSimone, *Proc. Natl. Acad. Sci. USA* **2008**, *105*, 11613.
[11] S. Bhaskar, J. Hitt, S. W. L. Chang, J. Lahann, *Angew. Chem.* **2009**, *121*, 4659; *Angew. Chem. Int. Ed.* **2009**, *48*, 4589.
[12] K. H. Roh, D. C. Martin, J. Lahann, *Nat. Mater.* **2005**, *4*, 759.
[13] J. R. Millman, K. H. Bhatt, B. G. Prevo, O. D. Velev, *Nat. Mater.* **2005**, *4*, 98.
[14] C. J. Hernandez, T. G. Mason, *J. Phys. Chem. C* **2007**, *111*, 4477.
[15] H. Zhang, J. K. Nunes, S. E. A. Gratton, K. P. Herlihy, P. D. Pohlhaus, J. M. DeSimone, *New J. Phys.* **2009**, *11*, 075018.
[16] D. Dendukuri, D. C. Pregibon, J. Collins, T. A. Hatton, P. S. Doyle, *Nat. Mater.* **2006**, *5*, 365.
[17] D. Dendukuri, S. S. Gu, D. C. Pregibon, T. A. Hatton, P. S. Doyle, *Lab Chip* **2007**, *7*, 818.
[18] J. H. Jang, D. Dendukuri, T. A. Hatton, E. L. Thomas, P. S. Doyle, *Angew. Chem.* **2007**, *119*, 9185; *Angew. Chem. Int. Ed.* **2007**, *46*, 9027.
[19] K. W. Bong, D. C. Pregibon, P. S. Doyle, *Lab Chip* **2009**, *9*, 863.
[20] D. Dendukuri, P. Panda, R. Haghgooie, J. M. Kim, T. A. Hatton, P. S. Doyle, *Macromolecules* **2008**, *41*, 8547.
[21] C. Simonnet, A. Groisman, *Anal. Chem.* **2006**, *78*, 5653.
[22] C. C. Chang, Z. X. Huang, R. J. Yang, *J. Micromech. Microeng.* **2007**, *17*, 1479.
[23] S. J. Choi, P. J. Yoo, S. J. Baek, T. W. Kim, H. H. Lee, *J. Am. Chem. Soc.* **2004**, *126*, 7744.
[24] T. Gervais, J. El-Ali, A. Gunther, K. F. Jensen, *Lab Chip* **2006**, *6*, 500.
[25] C. Simonnet, A. Groisman, *Appl. Phys. Lett.* **2005**, *87*, 114104.
[26] S. K. Yoon, M. Mitchell, E. R. Choban, P. J. A. Kenis, *Lab Chip* **2005**, *5*, 1259.
[27] J. B. Leach, C. E. Schmidt, *Biomaterials* **2005**, *26*, 125.

